Nuclear Engineering and Technology 53 (2021) 2977–2981

Contents lists available at ScienceDirect

Nuclear Engineering and Technology

journal homepage: www.elsevier.com/locate/net

Original Article

Corrosion fatigue crack growth behavior of 316LN stainless steel in high-temperature pressurized water

Ziyu Zhang, Jibo Tan, Xinqiang Wu*, En-Hou Han, Wei Ke

CAS Key Laboratory of Nuclear Materials and Safety Assessment, Liaoning Key Laboratory for Safety and Assessment Technique of Nuclear Materials, Institute of Metal Research, Chinese Academy of Sciences, Shenyang, 110016, PR China

ARTICLE INFO

Article history:
Received 30 November 2020
Received in revised form
18 March 2021
Accepted 18 March 2021
Available online 30 March 2021

Keywords:
Stainless steel
Fatigue crack growth rate
High-temperature water
Environmental assisted damage

ABSTRACT

Corrosion fatigue crack growth (FCG) behavior of 316LN stainless steel was investigated in high-temperature pressurized water at different temperatures, load ratios ($R = K_{max}/K_{min}$) and rise times (t_R). The environmental assisted effect on FCG rate was observed when both the R and t_R exceeded their critical values. The FCG rate showed a linear relation with stress intensity factor range (ΔK) in double logarithmic coordinate. The environmental assisted effect on FCG rate depended on the ΔK and quantitative relations were proposed. Possible mechanisms of environmental assisted FCG rate under different testing conditions are also discussed.

1. Introduction

316LN stainless steel has been widely used as the key structural materials in the primary circuit pipeline in nuclear power plants (NPPs). Operating experiences of NPPs and accumulative research data reveal that the fatigue resistance of stainless steels may be significantly influenced by high-temperature pressurized water environments [1–5]. Crack growth behavior dominates the fatigue damage process after crack initiation. Studies on corrosion fatigue crack growth behavior in high-temperature pressurized water environments have been focused on the effects of mechanical parameters, water chemistry and material parameters [4–10]. The environmental assisted fatigue crack growth (FCG) is obvious when the loading frequency between 3×10^{-6} to 0.1 Hz [5]. Below 150 °C, no obvious enhancement of FCG is observed for stainless steels, which is consistent with low cycle fatigue behavior in high-temperature pressurized water [5,11,12]. Studies on the FCG behavior of low-alloy steels in high-temperature water find that the assisted effect of FCG rate exist in a certain range of ΔK, and the range of ΔK varies with load ratio ($R = K_{max}/K_{min}$) [8,13,14]. When ΔK exceeds 2 MPa $m^{0.5}$ the environmental assisted effect on FCG rate of low-alloy steels decreases with increasing ΔK, and the range of ΔK varies with loading rate, the maximum of K and sulfur content [8]. But the crack growth behavior still needs further study when ΔK exceeds 20 MPa $m^{0.5}$. Also, the range of ΔK among which the environmental assisted effect is obvious changed with sulfur content of low alloy steels [14]. Therefore, the assisted effect of FCG rate of stainless steels in high-temperature water may also be different at different ΔK values. More detailed work is needed to determine the influence of ΔK on FCG behavior of stainless steels in high-temperature water. It has been reported that the environmental assisted effect of high-temperature water on FCG rate increases with increasing R when the R below the critical value (0.95 for low-alloy steels and 0.9 for stainless steels) [5,8]. At high R values ($\geq$0.95) crack arrest has been observed for low-alloy steels in high-temperature water. Disappearance of environmental assisted effect has also been observed for stainless steels and nickel base alloys in high-temperature water [10,15]. The quantitative relations between the FCG rate and ΔK at different R values are still not systematically studied when R below the critical value. Also, the related mechanism of environmental assisted effect on FCG rate at different R values is not clear.

The main purpose of the present work is to investigate the FCG behavior of 316LN stainless steel in high-temperature pressurized water under the conditions of different water temperatures, rise times (t_R) and R values. The objectives are to identify the regularities of FCG rate in high-temperature water and obtain the relationship between the FCG rate and ΔK under the different testing

* Corresponding author.
E-mail address: xqwu@imr.ac.cn (X. Wu).

https://doi.org/10.1016/j.net.2021.03.016

conditions. The FCG rate in high-temperature water was also compared with the ASME XI FCG curve in air. Special attention was paid to the link between environmental damage and the assisted effect on FCG rate of 316LN stainless steel in high-temperature water.

2. Experimental

2.1. Material and specimen

Table 1 is the compositions of 316LN stainless steel used for the present work. According to ASTM E647-08, compact tension (CT) specimens with a thickness of 15 ± 0.25 mm were used for FCG tests in high-temperature pressurized water.

2.2. FCG test

CT specimens were tested with an electro-servo hydraulic fatigue test machine equipped with a high-temperature pressurized recirculating water loop. The CT specimens were sealed in an 11 L stainless steel autoclave. A pressure-balance axle was used in the testing system to eliminate the influence of the high pressure on the load measurement. The water chemistry is summarized in Table 2. The fluctuations of temperature and dissolved oxygen (DO) were well controlled within ±0.5 °C and ±1 ppb respectively (the constant value was 1 ppb during CF test). In order to keep DO below 5 ppb, pure nitrogen was constantly purged into the water tank. Before FCG test, pre-cracking was performed in air to a crack length increment of about 2 mm by triangle waveform at a maximum stress intensity factor (K_{max}) less than 18 MPa $m^{0.5}$ and a frequency of 20 Hz. The crack length of CT specimen was in-situ monitored using reversed direct current potential drop (DCPD) technique. 316 stainless steel current and potential probe leads were spot-welded to CT specimen to measure crack length. The leads were covered with Teflon heat shrinkable tube and zirconia tube for isolation. Zirconia bushings and spacers were used to isolate the CT specimen from clamps. The FCG test in high-temperature pressurized water was performed under load control with a saw tooth waveform (rise time t_R = 10, 30 s; decline time t_D = 10 s). The ΔK level, load ratio R and t_R are summarized in Table 3.

3. Results

3.1. Effect of water temperature on FCG rate of 316LN stainless steel

Fig. 1 shows the FCG rate of 316LN stainless steel with t_R of 10 s. The FCG rate was found to be distributed around the ASME XI FCG curve [16] for stainless steels in different temperature water. The ASME XI FCG curve for stainless steels is expressed by the following equations [16]:

$$da/dN_{Air} = C_0 S(R)\ \Delta K^{3.3} \quad (1)$$

$$log\ (C_0) = -8.714 + 1.34 \times 10^{-3} T - 3.34 \times 10^{-6} T^2 + 5.95 \times 10^{-9} T^3 \quad (2)$$

$$S(R) = 1 + 1.8R \text{ for } R \leq 0.79 \quad (3)$$

$$S(R) = -43.35 + 57.97R \text{ for } 0.79 < R < 1 \quad (4)$$

Table 1
Composition of 316LN stainless steel (wt.%).

Cr	Ni	Mo	C	Si	Mn	S	P	N	Fe
16.96	13.07	2.23	0.014	0.29	1.40	0.003	0.014	0.12	Bal.

Table 2
Water chemistry specifications.

Temperature	120, 220, 320 °C
Pressure	0.5, 3, 12 MPa
DO	<5 ppb (by weight)

Table 3
Load specifications.

R	ΔK (MPa·$m^{0.5}$)	t_R (s)	Temperature (°C)
0.05	17 to 35	10, 30	120, 220, 320
0.4	12 to 24	10, 30	320
0.7	11 to 13	30	320

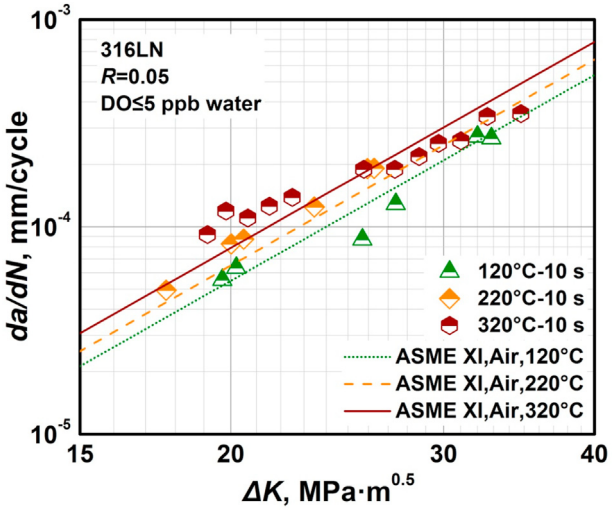

Fig. 1. FCG rate of 316LN stainless steel with t_R of 10 s.

When t_R increases to 30 s the environmental assisted effect on FCG rate is observed (Fig. 2). The environmental assisted effect is more obvious in 220 and 320 °C water. The dependence of da/dN on ΔK can be described as follows.

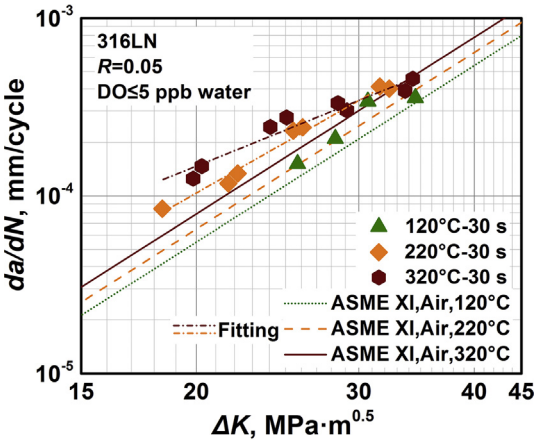

Fig. 2. FCG rate of 316LN stainless steel with t_R of 30 s.

220 °C-R0.05- t_R 30 s: $log\ (da/dN) = 2.956log\ (\Delta K) - 7.832$ (5)

320 °C-R0.05- t_R 30 s: $log\ (da/dN) = 2.098log\ (\Delta K) - 6.562$ (6)

3.2. Effect of rise time on FCG rate of 316LN stainless steel

Fig. 3 shows the FCG rate of 316LN stainless steel at different t_R in 120 °C water. The FCG rate distributes around the ASME crack growth rate curve in air. In 120 °C water the incense of t_R do not accelerate the FCG rate which is similar to the result of FCG rate in air [11]. In 220 °C (Fig. 4) and 320 °C (Fig. 5) water, the FCG rate at $t_R = 30$ s is higher than that at $t_R = 10$ s. This indicates that environmental assisted effect on FCG rate is more obvious at long t_R conditions when water temperature exceeds 220 °C.

3.3. Effect of load ratio on FCG rate of 316LN stainless steel

Figs. 6 and 7 show the FCG rate of 316LN stainless steel at different R values in 320 °C water with $t_R = 10$ s and $t_R = 30$ s. The FCG rate increases with increasing R value from 0.05 to 0.7 when the t_R is 10 s. When the t_R is 30 s the FCG rate at $R = 0.4$ is higher than that at $R = 0.05$ which is similar to the tendency of t_R at 10 s. The dependence of da/dN on ΔK at different R values and t_R can be described as follows.

320 °C-R0.4- t_R 10 s: $log\ (da/dN) = 2.020log\ (\Delta K) - 6.211$ (7)

320 °C-R0.7- t_R 10 s: $log\ (da/dN) = 2.311log\ (\Delta K) - 6.316$ (8)

320 °C-R0.4- t_R 30 s: $log\ (da/dN) = 2.189log\ (\Delta K) - 6.338$ (9)

Compared with ASME FCG curve in air, the increase of FCG rate is more obvious at high R value. Fig. 8 shows the fatigue striations on fracture surface in high-temperature water and air environments at different R values. Clear fatigue striation peaks are observed on fracture surface in air at different R values. In high-temperature water, the fatigue striation peaks are still clear when the R is 0.05 and corrosion products are observed on fatigue striations (Fig. 8a). By contrast, the fatigue striations are less distinct when the R is 0.4 (Fig. 8b).

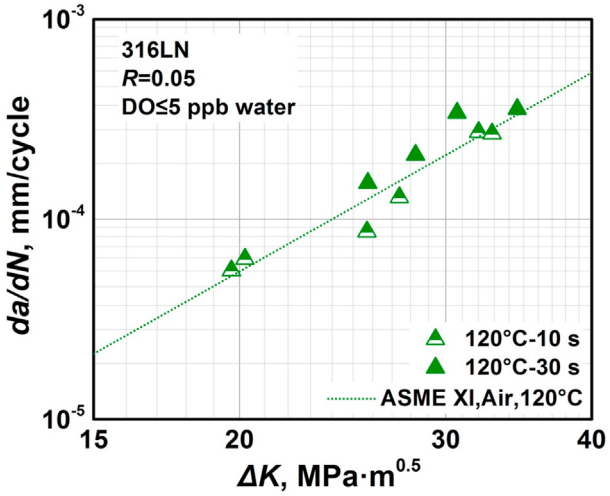

Fig. 3. FCG rate of 316LN stainless steel at different t_R in 120 °C water.

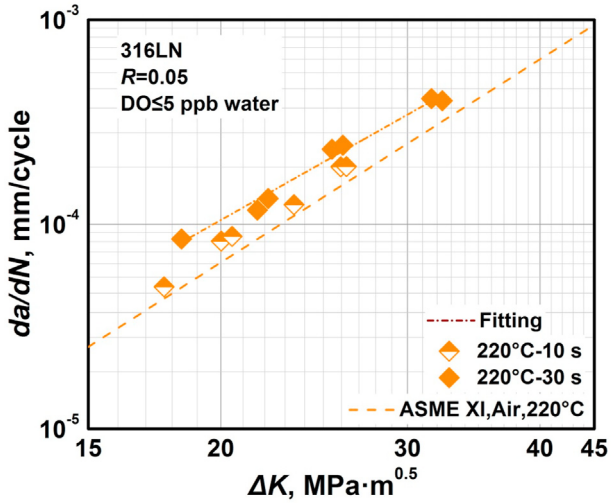

Fig. 4. FCG rate of 316LN stainless steel at different t_R in 220 °C water.

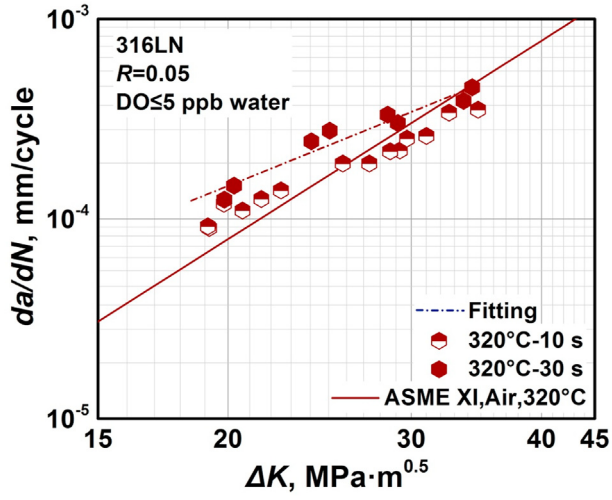

Fig. 5. FCG rate of 316LN stainless steel at different t_R in 320 °C water.

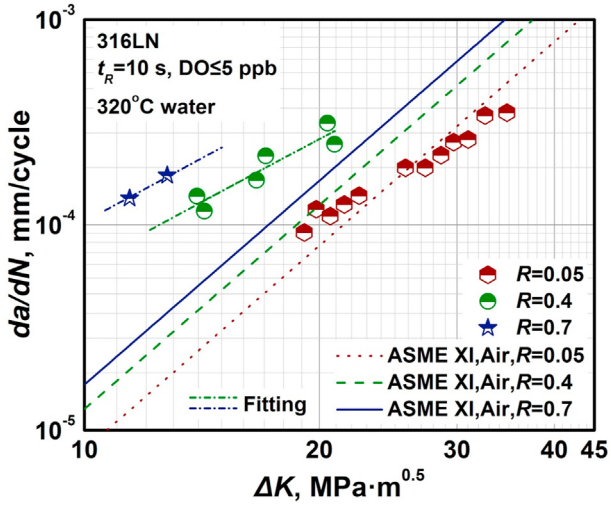

Fig. 6. FCG rate of 316LN stainless steel at different R values in 320 °C water with $t_R = 10$ s.

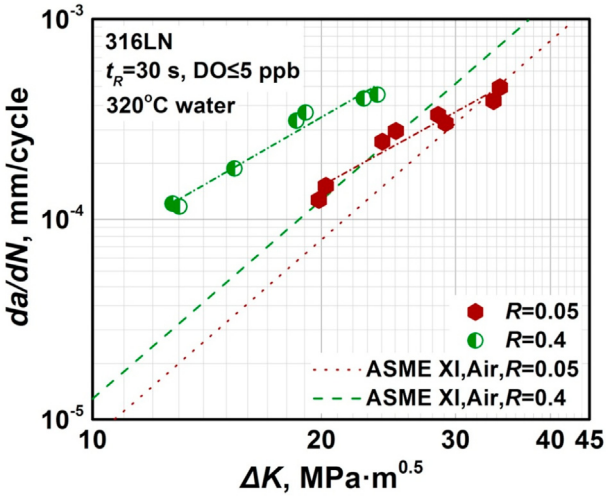

Fig. 7. FCG rate of 316LN stainless steel at different R values in 320 °C water with t_R = 30 s.

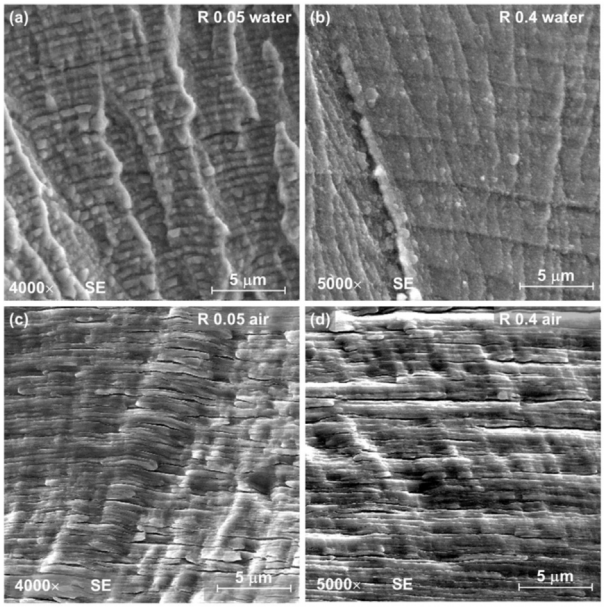

Fig. 8. Fatigue striations on fracture surface in high-temperature water and air environments at different R values.

4. Discussion

4.1. Environmental assisted effect on FCG in high-temperature pressurized water

Figs. 1–5 indicate that the environmental assisted effect on FCG becomes obvious when water temperature exceeds 220 °C and t_R exceeds 30 s under the condition of $R = 0.05$. And the threshold of water temperature on FCG rate acceleration is related to t_R. It is well known that the corrosion fatigue crack process is a time dependent process under certain conditions [17]. The environmental assisted effect on FCG is related to the interaction time of corrosion process during deformation [11]. At long t_R condition, long time immersion of crack tip material during crack opening gives enough time for the corrosion process to occur. And it should be noted that the environmental assisted effect is also related to ΔK value. As shown in Fig. 2, in 220 °C and 320 °C water the increase of FCG rate decreases with increasing ΔK and distributes around the ASME XI FCG curve when ΔK exceeds 30 MPa $m^{0.5}$. The environmental assisted effect can be described by FCG correction factor F_c which is defined as:

$$F_c = (da/dN_{water}) / (da/dN_{air}) \quad (10)$$

According to equations (1) to (6) and (10), the F_c in 220 °C and 320 °C water can be obtained as follows.

$$220\ ^\circ C\text{-R0.05- } t_R \text{ 30 s: } log\ (F_c) = 0.648\text{-}0.344log\ (\Delta K) \quad (11)$$

$$320\ ^\circ C\text{-R0.05- } t_R \text{ 30 s: } log\ (F_c) = 1.833\text{-}1.202log\ (\Delta K) \quad (12)$$

According to equations (11) and (12), the F_c in 220 °C and 320 °C water has a linear relation with ΔK at $R = 0.05$ and $t_R = 30$ s condition. And F_c increases with the decreasing of ΔK. During fatigue process the plastic deformation of metal at crack tip increases with increasing ΔK. It has been reported that the dislocation structure changed from planner slip to wavy slip with plastic deformation increasing [12]. Planner slip could produce more obvious strain localization nearby the crack tip and promote the synergy of corrosion damage and mechanical damage, which in turn assists the FCG rate of 316LN stainless steel in high temperature water. Therefore, the environmental assisted effect on FCG rate increases with decreasing ΔK.

4.2. Load ratio dependence of FCG rate in high-temperature pressurized water

According to Figs. 6 and 7, the environmental assisted effect is more obvious at high R value. The FCG correction factor F_c can be obtained as follows.

$$320\ ^\circ C\text{-R0.4- } t_R \text{ 10 s: } log\ (F_c) = 2.184\text{-}1.280log\ (\Delta K) \quad (13)$$

$$320\ ^\circ C\text{-R0.7- } t_R \text{ 10 s: } log\ (F_c) = 2.079\text{-}0.989log\ (\Delta K) \quad (14)$$

$$320\ ^\circ C\text{-R0.4- } t_R \text{ 30 s: } log\ (F_c) = 2.057\text{-}1.111log\ (\Delta K) \quad (15)$$

The F_c at different R values was also connected with ΔK, and linear increasing with the decrease of ΔK. It is reported that hydrogen plays an important role in assisted FCG rate in high-temperature water [12,18–20]. Crack opening becomes more obvious with increasing R, thus the hydrogen generated during corrosion process has enough time to diffuse into the metal near the crack tip. This will introduce intense hydrogen damage and accelerate the FCG rate. Kanezaki [21] reported that hydrogen could increase the localized plastic deformation around the crack tip. With the increasing of localized plastic deformation, the formation of fatigue striations became difficult and the striation height decreased. Fig. 8 shows the fatigue striations on fracture surface in high-temperature water and air environments at different R values. Clear fatigue striation peaks are observed on fracture surface in air at different R value. In high-temperature water, the fatigue striation peaks are still clear when the R is 0.05 and corrosion products are observed on fatigue striations (Fig. 8a). By contrast, the fatigue striations are less distinct when the R is 0.4 (Fig. 8b). This indicated that the effect of hydrogen is more obvious under the high R value conditions. When hydrogen is absorbed into the crack tips during fatigue process, the mobility of dislocation can be improved [22,23] and lead to more obvious planar slip. The formation of fatigue striation is due to the dislocation slip along different slip systems during repeated blunting and sharpening of the crack tip. Since the planar slip becomes more obvious, the fatigue striation is not

distinct under the high R value conditions in high-temperature water. Also, higher R value results in higher stress level around the crack tip, therefore the metal around the crack tip have high chemical activity. This in turn promotes the interaction between environmental damage and mechanical damage in high-temperature water. Thus obvious environmental assisted effect on FCG rate is observed under high R value conditions.

5. Conclusion

FCG behavior of 316LN stainless steel in high-temperature water under the conditions of different temperatures, rise times and R values was investigated. The regularities of FCG under different testing conditions were analyzed and the related mechanisms were discussed. FCG correction factor F_c was used to describe the environmental assisted effect of high-temperature pressurized water environment. The following conclusions could be drawn.

(1) The difference of FCG behavior of 316LN stainless steel in high-temperature pressurized water at different water temperature and R value with small changes of t_R was distinguished. And quantitative relations between FCG rate and ΔK at different water temperature, R value and t_R were proposed.
(2) Under the present test conditions, the threshold of water temperature and t_R were 220 °C and 30 s respectively when R was 0.05. And the threshold of water temperature on FCG rate acceleration was related to t_R. The environmental assisted effect on FCG rate was also related to ΔK value. Quantitative relations between FCG correction factor F_c and ΔK were obtained.
(3) Under same ΔK and t_R conditions, the increase of FCG rate in high-temperature water became more obvious when the R value increased. Less distinct fatigue striations formed on fatigue fracture surfaces was observed. This can be regarded as the circumstantial evidence of obvious hydrogen effect when the R value increases.

Declaration of competing interest

The authors declare that they have no known competing financial interests or personal relationships that could have appeared to influence the work reported in this paper.

Acknowledgements

This study was jointly supported by the Natural Science Foundation of Liaoning Province of China (2020-BS-005), the Open Foundation of CAS Key Laboratory of Nuclear Materials and Safety Assessment (292020000038), the National Science and Technology Major Project (2017ZX06002003-004-002) and CNNC Science Fund for Talented Young Scholars.

References

[1] L. Dong, E.-H. Han, Q. Peng, W. Ke, L. Wang, Environmentally assisted crack growth in 308L stainless steel weld metal in simulated primary water, Corrosion Sci. 117 (2017) 1–10.
[2] J. Tan, X. Wu, E.-H. Han, X. Liu, X. Xu, H. Sun, The effect of dissolved oxygen on fatigue behavior of Alloy 690 steam generator tubes in borated and lithiated high temperature water, Corrosion Sci. 102 (2016) 394–404.
[3] J. Gao, J. Tan, M. Jiao, X. Wu, L. Tang, Y. Huang, Role of welding residual strain and ductility dip cracking on corrosion fatigue behavior of Alloy 52/52M dissimilar metal weld in borated and lithiated high-temperature water, J. Mater. Sci. Technol. 42 (2020) 163–174.
[4] K. Chen, D. Du, L. Zhang, P.L. Andresen, Corrosion fatigue crack growth behavior of alloy 690 in high-temperature pressurized water, Corrosion 73 (2017) 724–733.
[5] H.P. Seifert, S. Ritter, H.J. Leber, Corrosion fatigue crack growth behaviour of austenitic stainless steels under light water reactor conditions, Corrosion Sci. 55 (2012) 61–75.
[6] J. Xiao, L. Chen, J. Zhou, S. Qiu, Y. Chen, Technical Note: corrosion fatigue crack growth of forged type 316NG austenitic stainless steel in 325°C water, Corrosion 74 (2017) 387–392.
[7] J. Huang, J. Yeh, R. Kuo, S. Jeng, M. Young, Fatigue crack growth behavior of reactor pressure vessel steels in air and high-temperature water environments, Int. J. Pres. Ves. Pip. 85 (2008) 772–781.
[8] H.P. Seifert, S. Ritter, Corrosion fatigue crack growth behaviour of low-alloy reactor pressure vessel steels under boiling water reactor conditions, Corrosion Sci. 50 (2008) 1884–1899.
[9] X. Lou, M.A. Othon, R.B. Rebak, Corrosion fatigue crack growth of laser additively-manufactured 316L stainless steel in high temperature water, Corrosion Sci. 127 (2017) 120–130.
[10] B. Young, X. Gao, T.S. Srivatsan, P. King, An investigation of the fatigue crack growth behavior of INCONEL 690, Mater. Sci. Eng., A 416 (2006) 187–191.
[11] O.K. Chopra, W.J. Shack, Effect of LWR Coolant Environments on Fatigue Life of Reactor Materials, NUREG/CR-6909, ANL-06/08, 2007.
[12] Z. Zhang, J. Tan, X. Wu, E.-H. Han, W. Ke, J. Rao, Effects of temperature on corrosion fatigue behavior of 316LN stainless steel in high-temperature pressurized water, Corrosion Sci. 146 (2019) 80–89.
[13] M. Itatani, T. Ogawa, C. Narazaki, T. Saito, Re-evaluation of fatigue crack growth curve for austenitic stainless steels in BWR environmenta, in: Proceedings of the ASME 2012 Pressure Vessels & Piping Conference, 2012. Toronto, Ontario, Canada, July 15-19.
[14] J.D. Atkinson, J. Yu, Z. Chen, Z. Zhao, Modelling of corrosion fatigue crack growth plateaux for RPV steels in high temperature water, Nucl. Eng. Des. 184 (1998) 13–25.
[15] T. Shoji, H. Takahashi, M. Suzuki, T. Kondo, A new parameter for characterizing corrosion fatigue crack growth, J. Eng. Mater. Technol. 103 (1981) 298–304.
[16] ASME Boiler and Pressure Vessel Code Section XI, ASME, New York, 2004.
[17] M. Yu, X. Xing, H. Zhang, J. Zhao, R. Eadie, W. Chen, J. Been, G.V. Boven, R. Kania, Corrosion fatigue crack growth behavior of pipeline steel under underload-type variable amplitude loading schemes, Acta Mater. 96 (2015) 159–169.
[18] Y. Oda, H. Noguchi, Observation of hydrogen effects on fatigue crack growth behaviour in an 18Cr-8Ni austenitic stainless steel, Int. J. Fract. 132 (2005) 99–113.
[19] J. Tan, X. Wu, E.-H. Han, W. Ke, X. Liu, F. Meng, X. Xu, Corrosion fatigue behavior of Alloy 690 steam generator tube in borated and lithiated high temperature water, Corrosion Sci. 89 (2014) 203–213.
[20] Y. Ogawa, D. Birenis, H. Matsunaga, A. Thøgersen, Ø. Prytz, O. Takakuwa, J. Yamabe, Multi-scale observation of hydrogen-induced, localized plastic deformation in fatigue-crack propagation in a pure iron, Scripta Mater. 140 (2017) 13–17.
[21] T. Kanezaki, C. Narazaki, Y. Mine, S. Matsuoka, Y. Murakami, Effects of hydrogen on fatigue crack growth behavior of austenitic stainless steels, Int. J. Hydrogen Energy 33 (2008) 2604–2619.
[22] H.K. Birnbaum, P. Sofronis, Hydrogen-enhanced localized plasticity—a mechanism for hydrogen-related fracture, Mater. Sci. Eng., A 176 (1994) 191–202.
[23] V.G. Gavriljuk, V.N. Shivanyuk, J. Foct, Diagnostic experimental results on the hydrogen embrittlement of austenitic steels, Acta Mater. 51 (2003) 1293–1305.